Autophagy 8:6, 883–892; June 2012; © 2012 Landes Bioscience

Dual roles of Atg8–PE deconjugation by Atg4 in autophagy

Zhong-Qiu Yu,[1] Tao Ni,[1] Bing Hong,[1] Hai-Yan Wang,[1] Fen-Jun Jiang,[1] Shenshen Zou,[2] Yong Chen,[2] Xi-Long Zheng,[3] Daniel J. Klionsky,[4] Yongheng Liang[2] and Zhiping Xie[1,*]

[1]School of Medicine; Nankai University; Tianjin, China; [2]College of Life Sciences; Nanjing Agricultural University; Nanjing, China; [3]Department of Biochemistry and Molecular Biology; Libin Cardiovascular Institute of Alberta; Smooth Muscle Research Group; University of Calgary; Calgary, Canada; [4]Life Sciences Institute and Departments of Molecular, Cellular and Developmental Biology, and Biological Chemistry; University of Michigan; Ann Arbor, MI USA

Keywords: autophagy, ubiquitin-like proteins, deconjugation, Atg4, Atg8

Abbreviations: Atg, autophagy-related; GABARAP, $GABA_A$ receptor-associated protein; GFP, green fluorescent protein; LC3, microtubule-associated protein 1 light chain 3; MVB, multivesicular body; PE, phosphatidylethanolamine; Ubl, ubiquitin-like; Vps, vacuolar protein sorting

Modification of target molecules by ubiquitin or ubiquitin-like (Ubl) proteins is generally reversible. Little is known, however, about the physiological function of the reverse reaction, deconjugation. Atg8 is a unique Ubl protein whose conjugation target is the lipid phosphatidylethanolamine (PE). Atg8 functions in the formation of double-membrane autophagosomes, a central step in the well-conserved intracellular degradation pathway of macroautophagy (hereafter autophagy). Here we show that the deconjugation of Atg8–PE by the cysteine protease Atg4 plays dual roles in the formation of autophagosomes. During the early stage of autophagosome formation, deconjugation releases Atg8 from non-autophagosomal membranes to maintain a proper supply of Atg8. At a later stage, the release of Atg8 from intermediate autophagosomal membranes facilitates the maturation of these structures into fusion-capable autophagosomes. These results provide new insights into the functions of Atg8–PE and its deconjugation.

Introduction

Autophagy is a major intracellular degradation pathway in eukaryotes.[1,2] By eliminating excessive or damaged cytoplasmic components, autophagy serves to maintain intracellular homeostasis. In multicellular organisms, autophagy is involved in diverse physiological processes, including development, immune defense and tumor suppression.[3,4] Unlike the proteasomal system, autophagy relies on lysosomal hydrolases for the degradation of its substrates. Since the hydrolases are segregated away from the rest of the cytoplasm by the lysosomal limiting membrane, a unique vesicle-mediated cargo delivery method is employed to overcome the topological barrier. These specialized double-membrane autophagosomes are formed through the maturation of precursor membrane sacs, termed phagophores. During this process, the concave side of a growing phagophore eventually becomes the lumenal side of an autophagosomal inner vesicle, sequestering any cytoplasmic materials in that region. Autophagosomes then fuse with lysosomes, leading to the degradation of their cargos.

The formation of autophagosomes depends on a set of well-conserved core autophagy machinery proteins.[2] In the *Saccharomyces cerevisiae* yeast model system, these proteins are encoded by the autophagy-related (*ATG*) genes. Among them, the Ubl protein Atg8 plays a critical role in the phagophore expansion process.[5-7] Atg8 is present on both sides of the phagophore.[8,9] Presumably on the concave side, it additionally functions as an anchoring point for cargo receptors.[10,11] The association of Atg8 with membrane structures requires a covalent modification that results in the conjugation of Atg8 to phosphatidylethanolamine (PE).[12] The reaction in vivo is catalyzed by the sequential actions of Atg7 (E1-like activating enzyme), Atg3 (E2-like conjugation enzyme) and the Atg12–Atg5-Atg16 complex (E3-like ligase).[12-14] The substrate of the conjugation reaction, a truncated Atg8 variant with a glycine residue exposed at the C terminus, comes from two sources: deconjugation of existing Atg8–PE or proteolytic processing of newly synthesized full-length Atg8. In both cases, the cleavage is catalyzed by a cysteine protease, Atg4.[15]

It is well known that the deconjugation activity of Atg4 is required for normal autophagy.[15] Details have been lacking, however, on the precise location and the functional significance of this reaction. In yeast, the formation of autophagosomes happens at specific sites close to the vacuole (the yeast analog of lysosomes), termed the phagophore assemply site (PAS).[16,17] In mutants that are defective in the targeting of Atg8 to the PAS, such as *atg16*Δ or *atg14*Δ, both conjugated and nonconjugated

*Correspondence to: Zhiping Xie; Email: zxie@nankai.edu.cn
Submitted: 04/14/11; Revised: 02/05/12; Accepted: 02/07/12
http://dx.doi.org/10.4161/auto.19652

forms of Atg8 are present, implying that the PAS might not be the sole site for these reversible reactions.[16]

Here we characterize the phenotype of deconjugation-defective cells. Our data demonstrate that deconjugation happens at both the PAS and non-PAS membranes, and that the reactions have different roles in the autophagy process.

Results

The role of deconjugation includes, but is not limited to, replenishing Atg8. The conjugation of Atg8 to PE results in the association of Atg8 with membrane structures, among which the phagophore is a prominent site under autophagy-inducing conditions.[8,12] Conversely, the deconjugation of Atg8−PE releases Atg8 back to the cytosol.[7,15] One apparent consequence of the deconjugation reaction is that some Atg8 can be recycled. If this is the main function of deconjugation, one prediction is that autophagy activity could be fully restored by introducing sufficient Atg8 in the absence of deconjugation. To test this possibility, we examined deconjugation-defective cells that have either normal or overexpressed levels of GFP-Atg8ΔR; the truncated Atg8 variant Atg8ΔR lacks the terminal arginine residue of nascent full-length Atg8, and thus does not require the initial processing by Atg4 for the subsequent conjugation reaction.

In *atg8*Δ cells expressing GFP-Atg8 under its endogenous promoter, the recruitment of GFP-Atg8 to perivacuolar autophagic structures could be clearly observed (**Fig. 1A**). These puncta correspond to primarily the PAS and in some cases completed autophagosomes.[7,16] In contrast, in *atg4*Δ *atg8*Δ cells expressing a normal level of GFP-Atg8ΔR, the number of GFP-Atg8 puncta was reduced, and the fluorescence of the puncta was much weaker (**Fig. 1A**). These data are consistent with the hypothesis that the supply of Atg8 to the PAS is reduced in the absence of deconjugation. In *atg4*Δ *atg8*Δ cells overexpressing GFP-Atg8ΔR (using the *CUP1* promoter), we observed slightly more, but significantly brighter, GFP-Atg8 puncta than in *atg8*Δ cells expressing the normal level of GFP-Atg8 (**Fig. 1A**), suggesting that the deficit in the supply of Atg8 was suppressed.

We then tested whether the recovery of the Atg8 supply translates into enhancement of autophagic flux. We first utilized the GFP-Atg8 processing assay, in which the generation of free GFP is indicative of autophagic delivery.[18] The expression of a normal level of GFP-Atg8ΔR in *atg4*Δ *atg8*Δ cells led to the appearance of a small amount of free GFP (relative to *atg8*Δ cells expressing GFP-Atg8) under nitrogen starvation conditions, indicating that the autophagy activity in deconjugation-defective cells was lower than normal (**Fig. 1B**). Although the overexpression of GFP-Atg8ΔR increased the amount of free GFP, the overall ratio of free GFP to GFP-Atg8 remained relatively stable (**Fig. 1B**, quantification data at the bottom), indicating that the boost in the amount of free GFP likely came from a higher spatial density of GFP-Atg8 rather than higher autophagic flux. To further verify this result, we examined the nonselective delivery of cytosol by autophagy using the more quantitative Pho8Δ60 assay.[19] Consistent with the western blotting data, the introduction of the GFP-Atg8ΔR variant led to a partial restoration of autophagy activity compared with the *atg4*Δ strain (**Fig. 1C**). In contrast, overexpressing GFP-Atg8ΔR produced no further improvement, suggesting that the autophagy defect in deconjugation-defective cells cannot be bypassed simply by supplying ample Atg8. Taken together, these data demonstrate that the function of deconjugation includes, but is not limited to, replenishing Atg8.

Deconjugation releases Atg8 from transient non-PAS reservoirs. The lack of deconjugation resulted in the accumulation of Atg8 in mostly the PE form (**Fig. S1**). Although some Atg8 was present at the PAS, the amount of Atg8 at the PAS in deconjugation-defective cells was lower than that in wild-type cells (**Fig. 1A**), indicating it is the accumulation of Atg8 at another site(s) that causes the reduced supply of Atg8. For this reason, we focused on a unique phenotype of deconjugation-defective cells: in this genetic background, a large population of GFP-Atg8 is present on the vacuolar membrane, which is not seen with wild-type cells (**Figs. 1A, 2A and B**). This phenotype suggests that the vacuolar membrane may be a transient reservoir of Atg8−PE that normally supplies the PAS. Alternatively, since the vacuole represents the terminal target for autophagosome fusion to complete the degradation process,[8,20] this phenomenon may represent an artifact accompanying the residual autophagy activity in deconjugation-defective cells; that is, a small number of autophagosomes still form and fuse with the vacuole, and the inability to release Atg8 molecules from the outer membrane results in their eventual accumulation on the vacuolar membrane. To examine the latter possibility, we additionally knocked out *ATG1*, *ATG14* or *ATG16* in the deconjugation-defective background. All three genes encode core autophagy machinery proteins that are essential for autophagosome formation.[2] As expected, the deletion of any one of these genes completely abolished autophagic flux as measured by the Pho8Δ60 assay (data not shown). Furthermore, consistent with the role of Atg14 and Atg16 in the targeting of Atg8 to the PAS,[16] deletion of either one of their encoding genes eliminated the appearance of the perivacuolar punctate GFP-Atg8 signal (**Fig. 2A**). In contrast, none of the deletions significantly affected the presence of GFP-Atg8 on the vacuolar membrane (**Fig. 2A**), suggesting that autophagosome formation is not required for delivering Atg8 to the vacuolar membrane and that the vacuolar membrane instead constitutes a transient reservoir of Atg8−PE or interconnects with such a reservoir.

A major route of protein trafficking that connects the vacuole with the rest of the endomembrane system is the vacuolar protein sorting (VPS) pathway.[21] To test whether Atg8 reached the vacuole through the VPS pathway or directly from the cytosol, we knocked out *VPS4* in deconjugation-defective cells. Vps4 is an ATPase functioning in the trafficking from the endosome to the vacuole.[22,23] Knocking out *VPS4* resulted in a significant increase in the number of GFP-Atg8 puncta in deconjugation-defective cells, as well as the appearance of "class E" compartments labeled by Snf7 or FM 4–64, even though little colocalization was observed between GFP-Atg8 and Snf7 (**Fig. 2B and C**; **Fig. S2**). Meanwhile, the accumulation of GFP-Atg8 on the vacuolar membrane remained prominent in the *vps4*Δ strain.

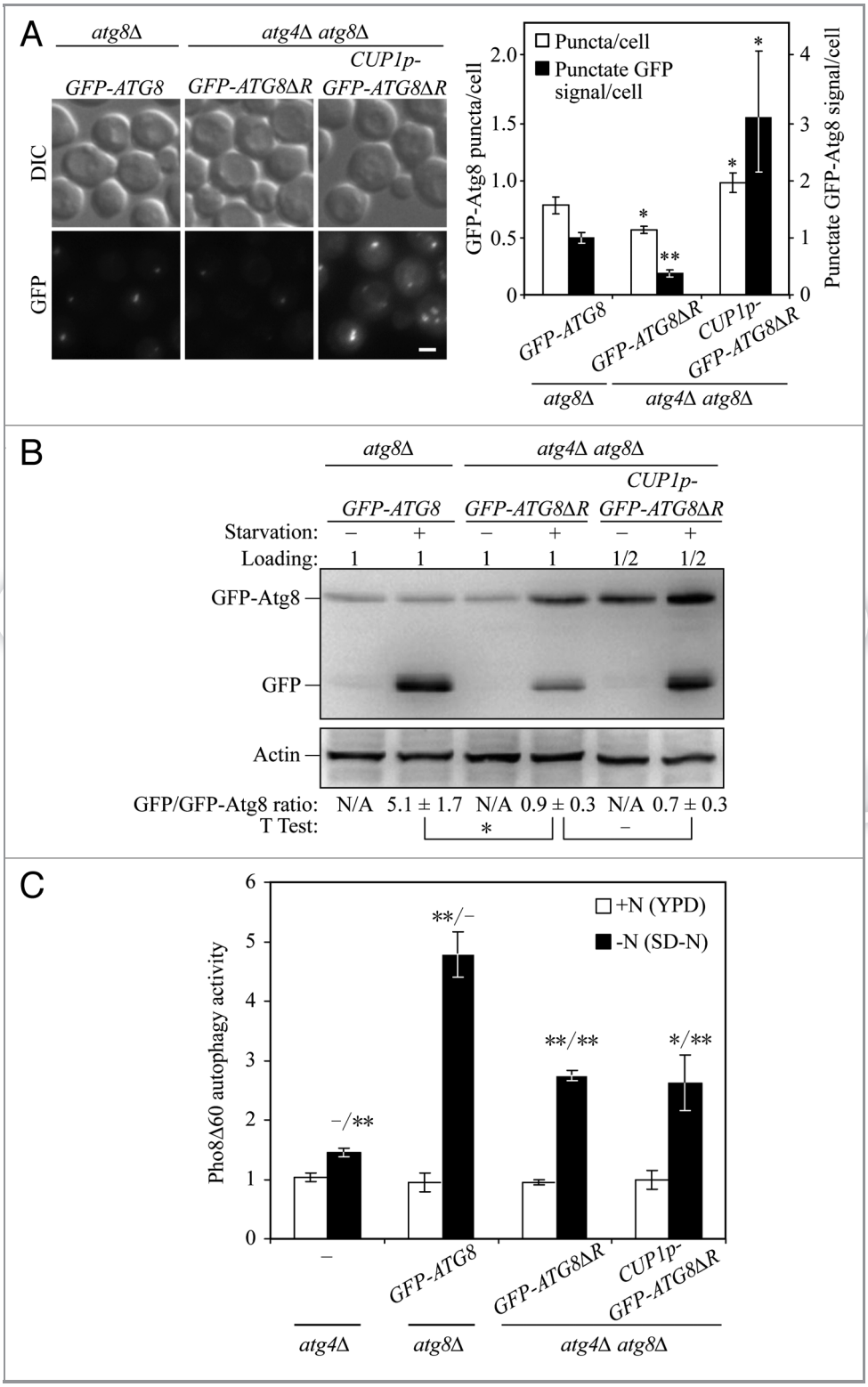

Figure 1. The role of deconjugation includes, but is not limited to, replenishing Atg8. (A) Deconjugation is necessary for maintaining supply of Atg8 to the PAS. Mid-log phase yeast cells were incubated in SD-N for 1 h, then fixed with 4% formaldehyde and imaged by fluorescence microscopy. Representative images are presented on the left. For the GFP signal, a stack of images was collected along the Z axis (step size: 0.5 μm) to cover the entire depth of the cells, then projected using maximum intensity to form one image. Scale bar: 2 μm. The quantification of the results for the number of GFP-Atg8 puncta per cell and the amount of punctate GFP-Atg8 fluorescence signal per cell are shown on the right. The experiments were repeated three times and at least 50 cells were quantified for each strain. For the fluorescence signal, the amount in *atg8Δ GFP-ATG8* cells was set to 1 and other values were normalized. Asterisks indicate significant p values from t-tests against data in *atg8Δ GFP-ATG8* cells: *$p < 0.05$, **$p < 0.01$. Error bar: standard error. (B and C) Overexpression of GFP-Atg8ΔR does not improve autophagic flux in deconjugation-defective cells. Yeast cells with the indicated genotype were grown to mid-log phase in YPD (rich medium), then incubated in SD-N (nitrogen starvation medium) for 4 h. (B) Turnover of GFP-Atg8. Cell lysates were analyzed by immunoblotting using antibody against GFP. The ratio of free GFP vs. GFP-Atg8 was quantified from three independent repeats. The values are listed as mean ± standard deviation. Asterisks indicate significant p values from t-test between marked groups: *$p < 0.05$. (C) Autophagic flux measured by the Pho8Δ60 assay. Average activity from YPD samples was set to 1 and other values were normalized. Asterisks indicate significant p values from t-tests against data in *atg4Δ* (before /) or *atg8Δ GFP-ATG8* (after /) cells: *$p < 0.05$, **$p < 0.01$. Error bar: standard deviation from three repeats.

These results suggest that the vacuolar population of Atg8 comes from both direct conjugation of cytosolic Atg8 and transport of Atg8–PE through a Vps4-dependent route.

Spatial restriction of Atg4 impedes a late stage in autophagosome maturation. The inability of overexpressed Atg8ΔR to improve autophagic flux in deconjugation-defective cells suggests that deconjugation is necessary for a late stage in autophagosome formation after enough Atg8 is recruited to the PAS (**Fig. 1**). As the overexpression concurrently increased the amount of Atg8 at both the vacuolar membrane and the PAS (**Fig. 1A**), this approach could not differentiate as to whether the persistence of Atg8 at the PAS or at the vacuolar membrane caused the delay at

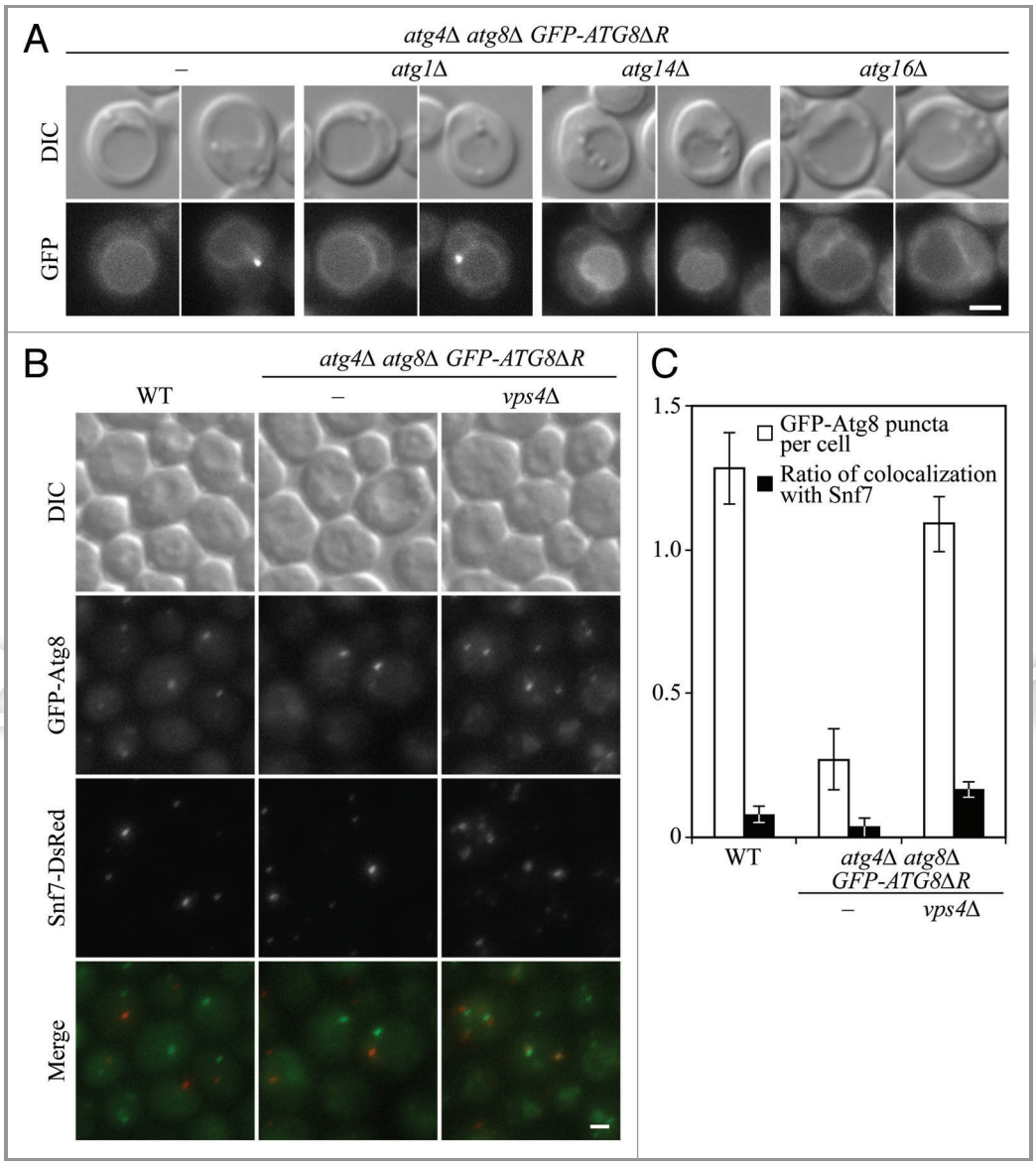

Figure 2. Deconjugation releases Atg8 from transient non-PAS reservoirs. (A) The accumulation of Atg8 on the vacuolar membrane in deconjugation-defective cells is independent of autophagosome formation. Mid-log phase yeast cells were incubated in SD-N for 1 h and imaged by fluorescence microscopy. For the GFP channel, representative images focusing on either the center of the cell or the perivacuolar GFP-Atg8 punctum (only if present) are shown. Scale bar: 2 μm. (B and C) Some Atg8 in deconjugation-defective cells arrives at the vacuolar membrane via a Vps4-dependent trafficking pathway. Cells were imaged as in **Figure 1A**. (B) Representative images. Scale bar: 2 μm. (C) Quantification results for the number of GFP-Atg8 puncta per cell and the ratio of GFP-Atg8 puncta that colocalize with Snf7-DsRed. The experiments were repeated three times and at least 50 cells were quantified for each strain. Error bar: standard error.

this stage. In order to isolate these two potential causes, we constructed a set of strains that express organelle-targeted Atg4 fusion proteins in the *atg4*Δ background (**Fig. S3**). Our rationale is that by targeting Atg4 to organelles, the activity of Atg4 can be spatially restricted, allowing us to dissect the roles of deconjugation at different sites.

In *atg4*Δ cells, the lack of initial processing of full-length Atg8 resulted in a diffuse GFP-Atg8 signal in the cytosol (**Fig. 3A**).[24] In *atg4*Δ cells expressing wild-type Atg4, normal PAS localization of GFP-Atg8 was restored. Similarly, the presence of vacuole-targeted Atg4 (Vac-Atg4) also allowed the formation of perivacuolar GFP-Atg8 puncta, indicating that the Atg4 domain is functional and is located on the cytosolic side of the vacuolar membrane. In contrast to *atg4*Δ *atg8*Δ cells expressing GFP-Atg8ΔR (**Fig. 2A**), there was no GFP-Atg8 accumulation on the vacuolar membrane (**Fig. 3A**), confirming that Vac-Atg4 was efficient at releasing Atg8 from this site (note that expressing the Atg8ΔR variant did not change the phenotype under such conditions, as the "ΔR bypass" becomes irrelevant in the presence of a functional Atg4 domain).

The average number of GFP-Atg8 puncta in Vac-Atg4-expressing cells was significantly higher than that in wild-type

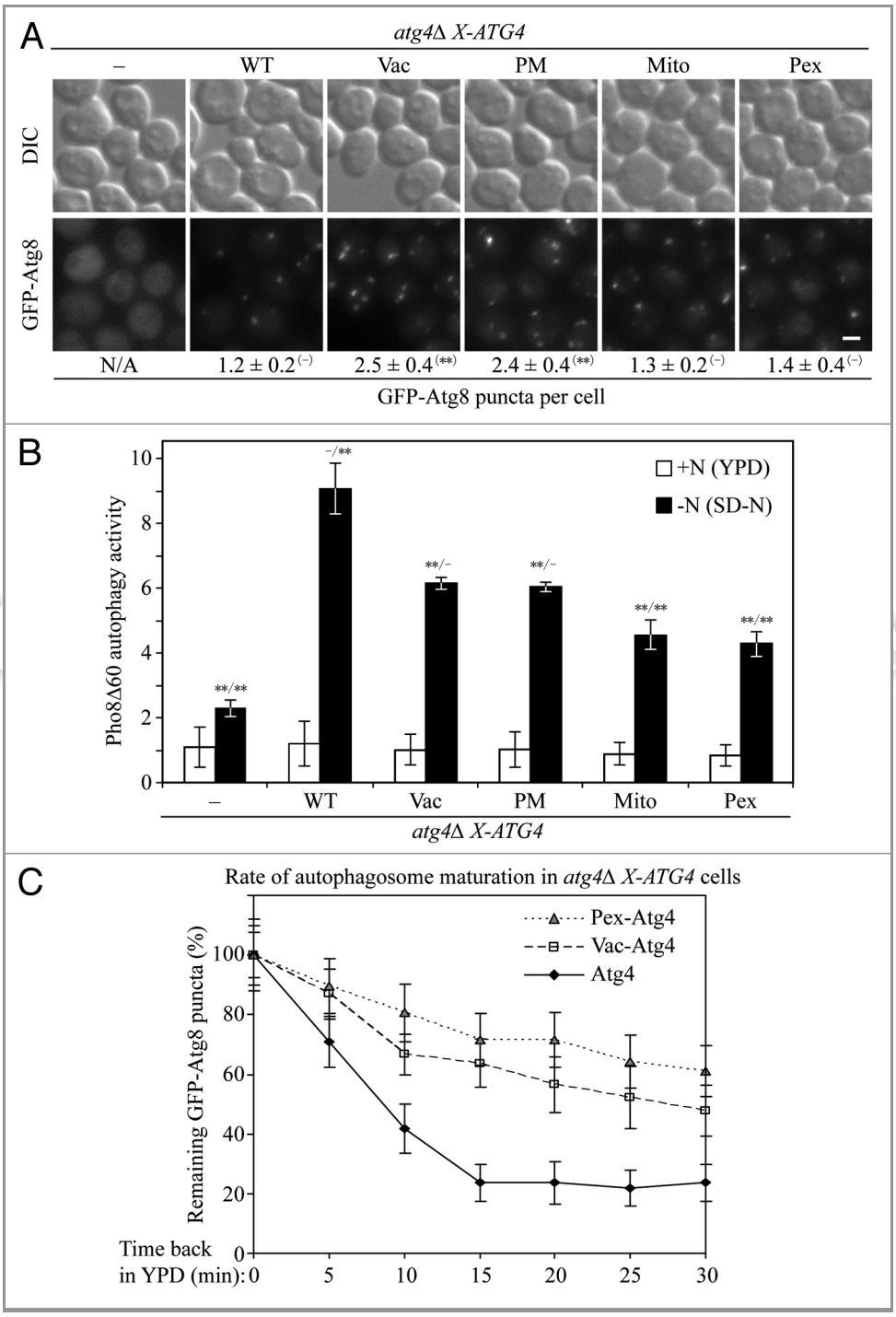

Figure 3. Organelle-targeted Atg4 selectively impedes late stages of autophagosome formation. (A) Vacuole-targeted Atg4 results in the accumulation of GFP-Atg8 puncta. *atg4*Δ cells expression full-length GFP-Atg8 were transformed with empty vector, vector expressing wild-type Atg4, or constructs targeting Atg4 to the vacuolar membrane (Vac-Atg4), plasma membrane (PM-Atg4), the mitochondria outer membrane (Mito-Atg4), or the peroxisomal membrane (Pex-Atg4). Cells were processed and analyzed by fluorescence microscopy as in **Figure 1A**. The average number of GFP-Atg8 puncta per cell was quantified from approximately 100 cells for each strain. The values are listed as mean ± standard error. Asterisks indicate significant p values from t-tests against data in WT cells: **p $<$ 0.01. Scale bar: 2 μm. (B) Organelle targeted Atg4 results in partial restoration of autophagic flux. Yeast cells carrying the indicated Atg4 constructs were processed and analyzed by the Pho8Δ60 assay as in **Figure 1C**. Asterisks indicate significant p values from t-tests against data in WT (before /) or Vac-Atg4 (after /) cells: **p $<$ 0.01. (C) Vacuole-targeted Atg4 delays the formation of fusion-capable autophagosomes. Mid-log phase yeast cells expressing GFP-Atg8 were incubated in SD-N for 1 h, then shifted back to YPD medium to shut off starvation-induced autophagy. At the indicated time points, cells were imaged by fluorescence microscopy and the number of GFP-Atg8 puncta was quantified. Error bar: standard error from approximately 50 cells.

Atg4 expressing cells (**Fig. 3A**). In contrast, the resulting autophagic flux measured by the Pho8Δ60 assay was lower (**Fig. 3B**). These results suggest that the increase in the number of GFP-Atg8 puncta does not come from enhanced autophagy; instead, it is caused by a delay in a late stage of autophagosome formation preceding the fusion of mature autophagosomes with the vacuole. To further verify such a delay, we experimented with tracking individual GFP-Atg8 puncta by time-lapse fluorescence microscopy; however, the existence of multiple GFP-Atg8 puncta in those cells made this analysis impractical. We instead performed a "pulse-chase" assay to examine the rate of GFP-Atg8 puncta turnover after autophagy inhibition (**Fig. 3C**). In wild-type cells, the majority of GFP-Atg8 puncta disappeared within 15 min after shifting from nitrogen starvation medium to nutrient rich medium. In contrast, in Vac-Atg4-expressing cells, approximately 50% of the puncta remained present even after 30 min, confirming that the half-life of these puncta was longer than that in wild-type cells.

To rule out the possibility that these additional puncta in Vac-Atg4 expressing cells were aberrant structures unrelated to autophagy, we tested whether their formation depended on Atg16, which mediates the targeting of Atg8 to the PAS.[14,16] In an *atg16*Δ background, no GFP-Atg8 puncta could be observed (**Fig. S4A**). In addition, in the *atg4*Δ cells expressing Vac-Atg4 the majority of the puncta disappeared after shifting back to YPD medium for 2 h (**Fig. S4B**). These data suggest that those puncta in Vac-Atg4 expressing cells are true intermediates in autophagosome formation.

Although significantly lower than wild-type Atg4-expressing cells, the recovery of autophagic flux in Vac-Atg4-expressing cells was notably higher than that in *atg4*Δ *atg8*Δ cells expressing GFP-Atg8ΔR (**Figs. 1C and 3B**). As the GFP-Atg8 puncta were motile (**Movie S1**),[7] we reasoned that the higher recovery resulted from random collision of the intermediate structures with the vacuole. To test the possibility that random contact of Atg8-containing intermediates with an organelle-bound Atg4 can partially rescue autophagy, we targeted Atg4 to the peroxisome (Pex-Atg4) and mitochondria (Mito-Atg4) (**Fig. S3**). Neither organelle has a known connection with either the vacuole or the PAS. Consistent with the "random contact" interpretation, both Pex-Atg4 and Mito-Atg4 lead to a small recovery of autophagic flux (**Fig. 3B**), and overexpression of Pex-Atg4 brought a further enhancement (**Fig. S5**). The half-life of GFP-Atg8 puncta in Pex-Atg4-expressing cells was longer than that of Vac-Atg4 (**Fig. 3C**), possibly because the vacuole (due to its large size) has a higher chance of contact with the Atg8-containing intermediate structures than do peroxisomes. In addition, there remained a faint ring of GFP signal around the vacuole with the peroxisome- and mitochondria-targeted constructs (**Fig. 3A**), indicating that Pex-Atg4 and Mito-Atg4 are less efficient at removing Atg8 from the vacuole than Vac-Atg4. We also tested a strain in which Atg4 was targeted to the plasma membrane (PM-Atg4) (**Fig. S3**). Overall, the phenotype of this strain was similar to that of Vac-Atg4 (**Fig. 3A and B**), possibly because the two sites are interconnected by vesicular transport.

Taken together, these data suggest that when Atg4 is restricted to the vacuolar membrane, intermediate Atg8-containing structures accumulate in the cytosol. These intermediates eventually fuse with the vacuole, presumably after random collision with the vacuole-targeted Atg4.

The presence of Atg8 on the vacuolar membrane per se does not impede autophagy. To further verify that it is the deconjugation at the PAS, not at the vacuole, that facilitates autophagosome maturation, we tried fusing Atg4 to two known integral membrane proteins at the PAS: Atg9 and Atg27.[25,26] Unfortunately, fusion of Atg4 to these two proteins rendered them nonfunctional (data not shown), precluding us from any further testing.

We instead experimented with targeting additional Atg8 to the vacuolar membrane (Atg8ΔGR-GFP-Vac) in wild-type cells to examine whether the presence of Atg8 on the vacuole per se can delay autophagy. To avoid being cleaved by endogenous Atg4, the Atg8 moiety in our construct lacks the last two amino acids (G and R) of full-length Atg8. Expressed in wild-type cells, the Atg8ΔGR-GFP-Vac chimeric protein was efficiently targeted to the vacuolar membrane (**Fig. 4A and B**). However, there was no noticeable difference in autophagic flux between this strain and a strain expressing the control construct (GFP-Vac) (**Fig. 4C**). These data suggest that other than serving as a temporary reservoir, the transient presence of Atg8 on the vacuole does not directly impede autophagy.

Discussion

In this study, we demonstrate that deconjugation of Atg8−PE by Atg4 plays dual roles in the autophagosome formation process (**Fig. 4D**). At the beginning stage of autophagosome formation, the release of Atg8 from non-PAS transient reservoirs by Atg4-dependent deconjugation was critical in maintaining a normal supply of Atg8 to the PAS. In the absence of deconjugation, the amount of Atg8 reaching the PAS was reduced. At a late stage of autophagosome formation, the release of Atg8 from the phagophore membrane facilitated the maturation of the phagophore into fusion-capable autophagosomes. In the absence of deconjugation, the defect at this stage could not be overcome by overexpressing Atg8ΔR. Targeting Atg4 to the vacuolar membrane in deconjugation-defective cells fully restored the supply of Atg8 to the PAS, although the defect in the later stage was only partially alleviated. Targeting additional Atg8 to the vacuolar membrane in wild-type cells did not affect autophagy significantly.

Our current data indicate that prior to reaching the PAS, some Atg8 molecules transiently associate with other endomembranes, including the vacuolar membrane. In the absence of deconjugation, Atg8−PE molecules from other compartments eventually reach the vacuole through a Vps4-dependent pathway (**Fig. 2B**). The transient nature of the association with non-PAS structures suggest that the balance of conjugation vs. deconjugation is regulated differently than that at the PAS. One notable dissimilarity here is that the association with the vacuole is not mediated by the E3 complex (**Fig. 2A**), which might give Atg4 an

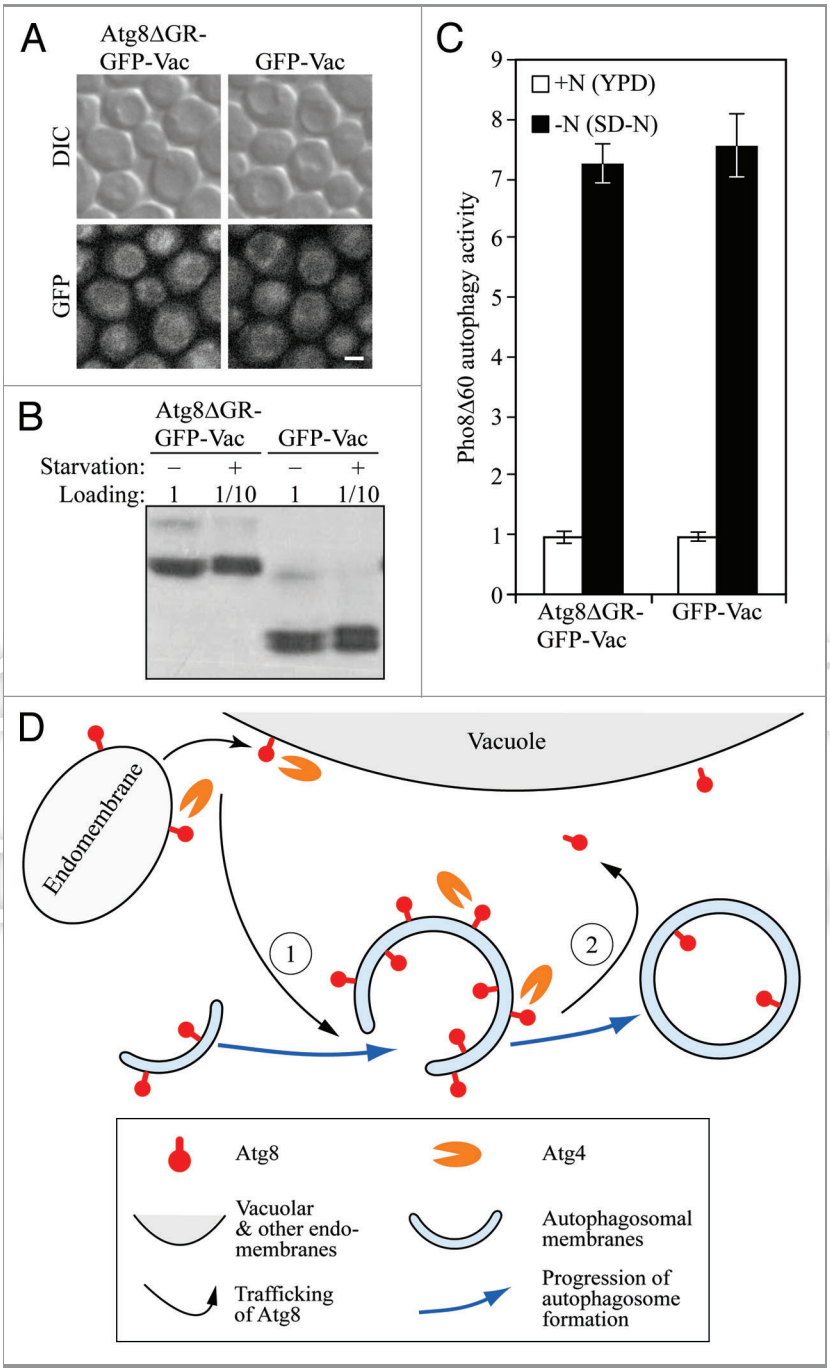

Figure 4. The presence of Atg8 on the vacuolar membrane per se does not impede autophagy. (A) Atg8ΔGR-GFP-Vac and GFP-Vac are efficiently targeted to the vacuolar membrane. Wild-type cells expressing either Atg8ΔGR-GFP-Vac or GFP-Vac were processed and analyzed by fluorescence microscopy as in **Figure 1A**. Scale bar: 2 μm. (B) Expression of Atg8ΔGR-GFP-Vac and GFP-Vac constructs. Samples were prepared as in **Figure 1B**. (C) The presence of Atg8 on the vacuolar membrane does not impede autophagy. Yeast cells carrying the indicated constructs were processed and analyzed by the Pho8Δ60 assay as in **Figure 1C**. (D) Schematic model of the dual roles of deconjugation in autophagosome formation: (1) at early stages of autophagosome formation, deconjugation supplies Atg8 to the PAS from transient reservoirs including the vacuole and other endomembranes; (2) at a later stage, deconjugation of Atg8 from the phagophore facilitates its maturation into a fusion-capable autophagosome. Although a phagophore is depicted here, the exact nature of the intermediate Atg8-containing structure is not known.

upper hand in shifting the balance toward deconjugation. Likewise, the instability of Atg8−PE at non-PAS sites may stem from the absence of other core machinery proteins, some of which may help protect Atg8−PE.[27] Considering that the surface area of the vacuole is approximately two orders of magnitude larger than that of the phagophore, the total amount Atg8 that transits through the vacuolar membrane would be significant. However, the physiological importance of this transient association is unclear.

The simplest interpretation would be that the association of Atg8 with other endomembranes is "off target," and that the deconjugation by Atg4 salvages those mislocalized Atg8 molecules. Alternatively, these non-PAS Atg8 molecules may be participating in other intracellular trafficking pathways. Consistent with such a possibility, two mammalian homologs of Atg8, GABARAP and LC3, have been reported to participate in the transport of $GABA_A$ receptors and in Toll-like receptor-mediated phagocytosis, respectively.[28,29]

In contrast to the role of deconjugation in supplying Atg8 to the PAS, the role of deconjugation in the maturation of the phagophore into fusion-capable autophagosomes cannot be bypassed by overexpressing Atg8ΔR (**Fig. 1**). In a certain sense, this result is similar to what has been recently shown for Doa4, a deubiquitination enzyme functioning in the multivesicular body (MVB) pathway.[23,30] Doa4 deubiquitinates cargo proteins prior to their sorting into the forming intralumenal vesicles of late endosomes. Accordingly, the lack of Doa4 results in decreased availability of ubiquitin monomers. Restoring the level of ubiquitin by overexpresssion does not rescue the sorting defect of ubiquitinated proteins in *doa4*Δ cells; instead, these proteins remain on the surface of endosomes and subsequently reach the vacuolar membrane.[30] It is well appreciated that modification by ubiquitin and Ubls constitutes important signals dictating the fate of target molecules. In many cases, the significance of the reverse process, that is, deconjugation, has been downplayed to be a matter of recycling. Together with the aforementioned Doa4 reports, our data suggest that the act of deconjugation can also serve as an important signal for the proper progression of the respective processes.

It is worth noting that aside from a common involvement of deconjugation, the formation processes of autophagosomes and MVBs have distinct differences. In the MVB pathway, it is a subset of cargo proteins that rely on the reversible ubiquitination for their entry into intralunemal vesicles. The formation of the intralumenal vesicles per se is not significantly affected by the lack of deconjugation.[31] In autophagosome formation, however, the target of Atg8 conjugation is PE in the membrane.[12] Unlike ubiquitin, Atg8 has a direct role in the formation of autophagosomes.[5,7] In the absence of deconjugation, the overall process of autophagy is notably reduced (**Fig. 1**).[15] Furthermore, there is no indication from existing publications that Atg8−PE is preferentially sorted to the inner vesicles of autophagosomes (which topologically correspond to the intralumenal vesicles of the MVB). Therefore the mechanism underlying the involvement of Atg4 in the late stage of autophagosome formation may differ significantly from that of Doa4 in the MVB pathway. In both pathways, further studies are needed to elucidate the precise details.

Materials and Methods

Yeast media. Nutrient-rich medium (YPD): 1% yeast extract, 2% peptone and 2% glucose; nitrogen starvation medium (SD-N): 2% glucose, and 0.17% yeast nitrogen base without amino acids and ammonium sulfate.

Construction of plasmids and strains. The plasmid expressing GFP-Atg8 under the control of the endogenous promoter [P_{1K}-GFP-Atg8(406)] was described previously.[7] The corresponding Atg8ΔR variant was constructed by site-directed mutagenesis using the follow primers: Forward, ACA TTT GGC TAG CAG TCT TTT ATA TG, Reverse, AGA CTG CTA GCC AAA TGT ATT TTC TC. To construct the plasmid overexpressing GFP-Atg8ΔR, CUP1p-GFP-Atg8ΔR(406), the promoter region of *CUP1* was amplified from genomic DNA using the following primers: Forward, TAG ATG GAG CTC CTA GTT AGA AAA AGA CAT T, Reverse, ATG TAT ACT AGT CGA TGA CTT CTA TAT GAT AT; the fragment was digested with SacI and SpeI, and inserted into P_{1K}-GFP-Atg8ΔR(406) vector treated with the same enzymes to replace the *ATG8* promoter.

To construct plasmid Atg4(404) expressing wild-type Atg4 under the control of the endogenous promoter, a DNA fragment containing the *ATG4* locus was amplified from genomic DNA using the following primers: Forward, CCC TGC GAG CTC TCT TGG AAT TGC TAC CAC GTG CAT G, Reverse, TTC GAC GCT AGC TTA TAC CAC CGT TGT CTT AAT CTT C; the fragment was digested with SacI and NheI, and inserted into the pRS404 vector backbone digested with SacI and SpeI.

The proteins used for targeting Atg4 to various organelles were selected according to the Yeast GFP Fusion database (http://yeastgfp.yeastgenome.org/). The fusion of Atg4 to the C terminus of Cot1 (Vac), Snq2 (PM), Msp1 (Mito) and Ant1 (Pex) was achieved through homologous recombination. DNA fragments containing *ATG4* and the *TRP1* marker gene were amplified from plasmid Atg4(404) using the following primers: for Cot1-Atg4, CGC TGC CAA CTG CAA CAC AGC TGA TTG CTT AGA GGA TCA TCG TAT AGG AGT GAT ATA CA and GTA TAT GTA CCG TAT AAC GAT TTT TAA AAG TAT TTA ATT CGA TTG TAC TGA GAG TGC AC; for Snq2-Atg4, TAT ACT CAA TAA AAT TAA AAA CAT AAG GAA AAA GAA GCA GCG TAT AGG AGT GAT ATA CA and CAG ATG AAT GCA CAA AAT GTT AAG TTA TCT GAA GCC CAC AGA TTG TAC TGA GAG TGC AC; for Msp1-Atg4, AAT GGA TGC TAC AAG TAC GTT GTC ATC TCA ACC TCT TGA TCG TAT AGG AGT GAT ATA CAT and GTG AAA ACT AGC TTA TCT GAT ATG ATA TGA TGC GTG AAT AGA TTG TAC TGA GAG TGC ACC; for Ant1-Atg4, TTT CCT AAA GCA CAA CGG ACA ACG CAA GCT GGC TTC CAC TCG TAT AGG AGT GAT ATA CA and TCT AAA CGC AAT GTG CTT ATT TCA GTA ATA GTA AGG ATT CGA TTG TAC TGA GAG TGC AC.

C-terminal tagging of Atg4 with GFP or 13Myc was constructed by homologous recombination. DNA fragments containing the homologous end sequence and appropriate tags were amplified from the pFA6a series of plasmids using the following primers: GGA AAC GGT AGG TAT TCA CAG TCC TAT TGA TGA AAA ATG CGC TTC GTA CGC TGC AGG TC and CAA GTA TAT ATG CTT ATG AAC TAG TGA ATT CCT TAC ACT AGC ATA GGC CAC TAG TGG AT.[32]

To construct the plasmid overexpressing Ant1-Atg4-13Myc, two fragments were amplified from genomic DNA using the following primer pairs: TTG GGT ACC GGG CCC GCC ATT

CAT GCA GCC TAC AC and TAG AGT TAA CAT TGA CGG CCG ATG TTG TTG AGG TGA ATT for the promoter of *YJR096W*; TCA CCT CAA CAA CAT CGG CCG TCA ATG TTA ACT CTA GAG TC and CAA AAG CTG GAG CTC TGA GAA AGC AAC CTG ACC TAC for the Ant1-Atg4-13Myc ORF. The fragments were inserted into pRS404 using ApaI, EagI and SacI sites. The resulting plasmid, YJR096Wp-Ant1-Atg4-13Myc(404), was linearized by NcoI before transforming into yeast cells.

To construct the plasmid targeting Atg8ΔGR-GFP to the vacuolar membrane, three fragments were inserted into pRS404, containing the *ATG8* promoter and ORF (lacking G and R), GFP ORF and *YML018C* ORF, respectively. The control construct contains the *ATG8* promoter, GFP ORF and *YML018C* ORF instead. The GFP ORF was amplified from plasmid FA6a-GFP-TRP1 using the following primers: GGC GGC CGC TCT AGA ACT AGT AAA GGA GAA GAA CTT TTC AC and GAT CGA CAG TCG AGC TCG ATCAGT TTT GTA TAG TTC ATC CAT GC. The rest of the fragments were amplified from genomic DNA using the following primers: AAA GCT GGA GCT CCA CCG CGG AAT CAT ACT TGA AGG ATG TA and AAG TTC TTC TCC TTT ACT AGT CAT GTC TCT AGT AAT TAT TTT ATT ATG ATT TTC / AAG TTC TTC TCC TTT ACT AGT AAA TGT ATT TTC TCC TGA GTA AGT GAC ATA, for the *ATG8* promoter and ORF/promoter only; ACT GAT CGA GCT CGA CTG TCG ATC ATG GTG TCG AAG GAT CAA AC and CTC GAG GTC GAC GGT ATC GAT GTA TGA AGC CAA CGA GAT AC for the *YML018C* ORF.

Gene knockout was performed as previously described.[32,33] When necessary, empty integration plasmids were transformed into appropriate yeast strains to ensure that strains being compared have the same auxotrophic genotype. Strains used in this study are listed in **Table 1**.

Fluorescence microscopy. For snap shots, yeast cells were fixed with 4% formaldehyde in PBS buffer for 30 min prior to observation. For time-lapse microscopy, a type of modified Petri dish with cover glass as the bottom was employed. The cover glass was treated with 1 mg/ml concanavalin A to immobilize yeast cells in liquid culture. Image stacks were captured to cover the entire depth of the cells at a step size of 0.5 μm per slice. The ambient temperature during the observation was approximately 22°C. The models of the microscopes are Olympus FV1000 and Nikon TiE.

Additional assays. Immunoblotting and the Pho8Δ60 assay were performed as described previously.[19,26]

Disclosure of Potential Conflicts of Interest

No potential conflicts of interest were disclosed.

Acknowledgments

This work was supported by National Key Basic Research Program of China grant 2011CB910100, National Natural Science Foundation of China grants 31171285 and 30971441 to Z.X., and National Institutes of Health grant GM53396 to D.J.K.

Table 1. Strains used in this study

Strain name	Genotype	Reference
SEY6210	*MATalpha his3Δ200 leu2–3,112 lys2–801 trp1-Δ901 ura3–52 suc2-Δ9 GAL+*	34
TN124	*MATalpha leu2–3,112 trp1 ura3–52 pho8::pho8Δ60 pho13Δ::LEU2*	19
WPHYD2	SEY6210 *atg4Δ::LEU2*	24
YHB101	YZX379 *SNF7::SNF7-DsRed-KAN*	This study
YHB103	YZX379 *vps4Δ::TRP1 SNF7::SNF7-DsRed-KAN*	This study
YHB104	SEY6210 *ura3::GFP-ATG8ΔR-URA3 SNF7::SNF7-DsRed-KAN*	This study
YNT401	WPHYD2 *trp1::ATG4–13Myc-HIS3MX6-TRP1*	This study
YNT402	WPHYD2 *ANT1::ANT1-ATG4–13Myc-HIS3MX6-TRP1*	This study
YNT403	WPHYD2 *MSP1::MSP1-ATG4–13Myc-HIS3MX6-TRP1*	This study
YNT404	WPHYD2 *COT1::COT1-ATG4–13Myc-HIS3MX6-TRP1*	This study
YNT405	WPHYD2 *SNQ2::SNQ2-ATG4–13Myc-HIS3MX6-TRP1*	This study
YNT407	YZX209 *SNQ2::SNQ2-ATG4-TRP1*	This study
YNT420	YZX209 *ANT1::YJR096Wp-ANT1-ATG4–13Myc-TRP1*	This study
YNT437	YZX200 *ura3::3HA-ATG8-URA3*	This study
YNT438	YZX200 *ura3::3HA-ATG8ΔR-URA3*	This study
YNT439	YZX206 *ura3::3HA-ATG8-URA3*	This study
YNT440	YZX206 *ura3::3HA-ATG8ΔR-URA3*	This study
YZQ01	YZX209 *ANT1::ANT1-ATG4-TRP1*	This study
YZQ03	YZX209 *COT1::COT1-ATG4-TRP1*	This study
YZQ02	YZX392 *ANT1::ANT1-ATG4-TRP1*	This study
YZQ04	YZX392 *COT1::COT1-ATG4-TRP1*	This study
YZQ07	YZX209 *MSP1::MSP1-ATG4-TRP1*	This study
YZQ08	YZX392 *MSP1::MSP1-ATG4-TRP1*	This study
YZQ09	YZX209 *trp1::ATG4-TRP1*	This study
YZQ10	YZX392 *trp1::ATG4-TRP1*	This study
YZQ215	YZX392 *SNQ2::SNQ2-ATG4-TRP1*	This study
YZQ231	YZQ10 *atg16Δ::HIS3MX6*	This study
YZQ233	YZQ04 *atg16Δ::HIS3MX6*	This study
YZQ235	YZQ215 *atg16Δ::HIS3MX6*	This study
YZQ234	YZQ08 *atg16Δ::HIS3MX6*	This study
YZQ232	YZQ02 *atg16Δ::HIS3MX6*	This study
YZQ310	WPHYD2 *trp1::ATG4-GFP-HIS3MX6-TRP1*	This study
YZQ311	WPHYD2 *COT1::COT1-ATG4-GFP-HIS3MX6-TRP1*	This study
YZQ314	WPHYD2 *SNQ2::SNQ2-ATG4-GFP-HIS3MX6-TRP1*	This study
YZQ313	WPHYD2 *MSP1::MSP1-ATG4-GFP-HIS3MX6-TRP1*	This study
YZQ312	WPHYD2 *ANT1::ANT1-ATG4-GFP-HIS3MX6-TRP1*	This study
YZX200	TN124 *atg8Δ::KAN*	7
YZX206	TN124 *atg4Δ atg8Δ*	This study
YZX209	TN124 *atg4Δ::URA3*	This study
YZX247	YZX200 *ura3::GFP-ATG8-URA3 TRP1*	7
YZX284	YZX206 *ura3::GFP-ATG8ΔR-URA3*	This study
YZX334	YZX284 *trp1::CUP1p-GFP-ATG8ΔR-TRP1*	This study
YZX379	SEY6210 *atg4Δ::LEU2 atg8Δ::HIS3 ura3::GFP-ATG8ΔR-URA3*	This study
YZX392	WPHYD2 *ura3::GFP-ATG8-URA3*	This study

Supplemental Materials

Supplemental materials may be found here:
www.landesbioscience.com/journals/autophagy/article/19652

References

1. Nakatogawa H, Suzuki K, Kamada Y, Ohsumi Y. Dynamics and diversity in autophagy mechanisms: lessons from yeast. Nat Rev Mol Cell Biol 2009; 10:458-67; PMID:19491929; http://dx.doi.org/10.1038/nrm2708
2. Xie Z, Klionsky DJ. Autophagosome formation: core machinery and adaptations. Nat Cell Biol 2007; 9:1102-9; PMID:17909521; http://dx.doi.org/10.1038/ncb1007-1102
3. Mizushima N, Levine B. Autophagy in mammalian development and differentiation. Nat Cell Biol 2010; 12:823-30; PMID:20811354; http://dx.doi.org/10.1038/ncb0910-823
4. Mizushima N, Levine B, Cuervo AM, Klionsky DJ. Autophagy fights disease through cellular self-digestion. Nature 2008; 451:1069-75; PMID:18305538; http://dx.doi.org/10.1038/nature06639
5. Nakatogawa H, Ichimura Y, Ohsumi Y. Atg8, a ubiquitin-like protein required for autophagosome formation, mediates membrane tethering and hemifusion. Cell 2007; 130:165-78; PMID:17632063; http://dx.doi.org/10.1016/j.cell.2007.05.021
6. Weidberg H, Shvets E, Shpilka T, Shimron F, Shinder V, Elazar Z. LC3 and GATE-16/GABARAP subfamilies are both essential yet act differently in autophagosome biogenesis. EMBO J 2010; 29:1792-802; PMID:20418806; http://dx.doi.org/10.1038/emboj.2010.74
7. Xie Z, Nair U, Klionsky DJ. Atg8 controls phagophore expansion during autophagosome formation. Mol Biol Cell 2008; 19:3290-8; PMID:18508918; http://dx.doi.org/10.1091/mbc.E07-12-1292
8. Kirisako T, Baba M, Ishihara N, Miyazawa K, Ohsumi M, Yoshimori T, et al. Formation process of autophagosome is traced with Apg8/Aut7p in yeast. J Cell Biol 1999; 147:435-46; PMID:10525546; http://dx.doi.org/10.1083/jcb.147.2.435
9. Kabeya Y, Mizushima N, Ueno T, Yamamoto A, Kirisako T, Noda T, et al. LC3, a mammalian homologue of yeast Apg8p, is localized in autophagosome membranes after processing. EMBO J 2000; 19:5720-8; PMID:11060023; http://dx.doi.org/10.1093/emboj/19.21.5720
10. Shintani T, Huang W-P, Stromhaug PE, Klionsky DJ. Mechanism of cargo selection in the cytoplasm to vacuole targeting pathway. Dev Cell 2002; 3:825-37; PMID:12479808; http://dx.doi.org/10.1016/S1534-5807(02)00373-8
11. Bjørkøy G, Lamark T, Brech A, Outzen H, Perander M, Overvatn A, et al. p62/SQSTM1 forms protein aggregates degraded by autophagy and has a protective effect on huntingtin-induced cell death. J Cell Biol 2005; 171:603-14; PMID:16286508; http://dx.doi.org/10.1083/jcb.200507002
12. Ichimura Y, Kirisako T, Takao T, Satomi Y, Shimonishi Y, Ishihara N, et al. A ubiquitin-like system mediates protein lipidation. Nature 2000; 408:488-92; PMID:11100732; http://dx.doi.org/10.1038/35044114
13. Hanada T, Noda NN, Satomi Y, Ichimura Y, Fujioka Y, Takao T, et al. The Atg12-Atg5 conjugate has a novel E3-like activity for protein lipidation in autophagy. J Biol Chem 2007; 282:37298-302; PMID:17986448; http://dx.doi.org/10.1074/jbc.C700195200
14. Fujita N, Itoh T, Omori H, Fukuda M, Noda T, Yoshimori T. The Atg16L complex specifies the site of LC3 lipidation for membrane biogenesis in autophagy. Mol Biol Cell 2008; 19:2092-100; PMID:18321988; http://dx.doi.org/10.1091/mbc.E07-12-1257
15. Kirisako T, Ichimura Y, Okada H, Kabeya Y, Mizushima N, Yoshimori T, et al. The reversible modification regulates the membrane-binding state of Apg8/Aut7 essential for autophagy and the cytoplasm to vacuole targeting pathway. J Cell Biol 2000; 151:263-76; PMID:11038174; http://dx.doi.org/10.1083/jcb.151.2.263
16. Suzuki K, Kirisako T, Kamada Y, Mizushima N, Noda T, Ohsumi Y. The pre-autophagosomal structure organized by concerted functions of *APG* genes is essential for autophagosome formation. EMBO J 2001; 20:5971-81; PMID:11689437; http://dx.doi.org/10.1093/emboj/20.21.5971
17. Kim J, Huang W-P, Stromhaug PE, Klionsky DJ. Convergence of multiple autophagy and cytoplasm to vacuole targeting components to a perivacuolar membrane compartment prior to de novo vesicle formation. J Biol Chem 2002; 277:763-73; PMID:11675395; http://dx.doi.org/10.1074/jbc.M109134200
18. Shintani T, Klionsky DJ. Cargo proteins facilitate the formation of transport vesicles in the cytoplasm to vacuole targeting pathway. J Biol Chem 2004; 279:29889-94; PMID:15138258; http://dx.doi.org/10.1074/jbc.M404399200
19. Noda T, Matsuura A, Wada Y, Ohsumi Y. Novel system for monitoring autophagy in the yeast *Saccharomyces cerevisiae*. Biochem Biophys Res Commun 1995; 210:126-32; PMID:7741731; http://dx.doi.org/10.1006/bbrc.1995.1636
20. Huang W-P, Scott SV, Kim J, Klionsky DJ. The itinerary of a vesicle component, Aut7p/Cvt5p, terminates in the yeast vacuole via the autophagy/Cvt pathways. J Biol Chem 2000; 275:5845-51; PMID:10681575; http://dx.doi.org/10.1074/jbc.275.8.5845
21. Bryant NJ, Stevens TH. Vacuole biogenesis in *Saccharomyces cerevisiae*: protein transport pathways to the yeast vacuole. Microbiol Mol Biol Rev 1998; 62:230-47; PMID:9529893
22. Babst M, Sato TK, Banta LM, Emr SD. Endosomal transport function in yeast requires a novel AAA-type ATPase, Vps4p. EMBO J 1997; 16:1820-31; PMID:9155008; http://dx.doi.org/10.1093/emboj/16.8.1820
23. Raiborg C, Stenmark H. The ESCRT machinery in endosomal sorting of ubiquitylated membrane proteins. Nature 2009; 458:445-52; PMID:19325624; http://dx.doi.org/10.1038/nature07961
24. Kim J, Huang W-P, Klionsky DJ. Membrane recruitment of Aut7p in the autophagy and cytoplasm to vacuole targeting pathways requires Aut1p, Aut2p, and the autophagy conjugation complex. J Cell Biol 2001; 152:51-64; PMID:11149920; http://dx.doi.org/10.1083/jcb.152.1.51
25. Reggiori F, Tucker KA, Stromhaug PE, Klionsky DJ. The Atg1-Atg13 complex regulates Atg9 and Atg23 retrieval transport from the pre-autophagosomal structure. Dev Cell 2004; 6:79-90; PMID:14723849; http://dx.doi.org/10.1016/S1534-5807(03)00402-7
26. Yen W-L, Legakis JE, Nair U, Klionsky DJ. Atg27 is required for autophagy-dependent cycling of Atg9. Mol Biol Cell 2007; 18:581-93; PMID:17135291; http://dx.doi.org/10.1091/mbc.E06-07-0612
27. Nair U, Cao Y, Xie Z, Klionsky DJ. Roles of the lipid-binding motifs of Atg18 and Atg21 in the cytoplasm to vacuole targeting pathway and autophagy. J Biol Chem 2010; 285:11476-88; PMID:20154084; http://dx.doi.org/10.1074/jbc.M109.080374
28. Chen ZW, Chang CS, Leil TA, Olsen RW. C-terminal modification is required for GABARAP-mediated GABA$_A$ receptor trafficking. J Neurosci 2007; 27:6655-63; PMID:17581952; http://dx.doi.org/10.1523/JNEUROSCI.0919-07.2007
29. Sanjuan MA, Dillon CP, Tait SW, Moshiach S, Dorsey F, Connell S, et al. Toll-like receptor signalling in macrophages links the autophagy pathway to phagocytosis. Nature 2007; 450:1253-7; PMID:18097414; http://dx.doi.org/10.1038/nature06421
30. Nikko E, André B. Evidence for a direct role of the Doa4 deubiquitinating enzyme in protein sorting into the MVB pathway. Traffic 2007; 8:566-81; PMID:17376168; http://dx.doi.org/10.1111/j.1600-0854.2007.00553.x
31. Richter C, West M, Odorizzi G. Dual mechanisms specify Doa4-mediated deubiquitination at multivesicular bodies. EMBO J 2007; 26:2454-64; PMID:17446860; http://dx.doi.org/10.1038/sj.emboj.7601692
32. Longtine MS, McKenzie A, 3rd, Demarini DJ, Shah NG, Wach A, Brachat A, et al. Additional modules for versatile and economical PCR-based gene deletion and modification in *Saccharomyces cerevisiae*. Yeast 1998; 14:953-61; PMID:9717241; http://dx.doi.org/10.1002/(SICI)1097-0061(199807)14:10<953::AID-YEA293>3.0.CO;2-U
33. Gueldener U, Heinisch J, Koehler GJ, Voss D, Hegemann JH. A second set of loxP marker cassettes for Cre-mediated multiple gene knockouts in budding yeast. Nucleic Acids Res 2002; 30:e23; PMID:11884642; http://dx.doi.org/10.1093/nar/30.6.e23
34. Robinson JS, Klionsky DJ, Banta LM, Emr SD. Protein sorting in *Saccharomyces cerevisiae*: isolation of mutants defective in the delivery and processing of multiple vacuolar hydrolases. Mol Cell Biol 1988; 8:4936-48; PMID:3062374